Finite Element Based Adaptive Modeling for Layered Composite Structures

P. M. Mohite * and

C. S. Upadhyay †

Department of Aerospace Engineering, Indian Institute of Technology Kanpur 208016 India

In this paper, an automatic adaptation of equivalent single layer and layerwise models in any region of the domain is devised using a simple modeling error estimator. The interelement jumps are used to define the modeling error indicator. The proposed modeling error indicator is found to be robust and methodology is very effective in reducing the modeling error. An initially damaged laminate is analysed for adaptive selection of models. The concept of sublayers introduced is found to be very effective to control the modeling error.

Keywords Equivalent single layer; layerwise; region-by-region model, sublayers, equilibrium based postprocessed transverse stresses, discretization error, modeling error estimation.

Nomenclature

$\mathbf{u}$	Generalized displacement field
p_{xy}	Inplane approximation order
p_z^i	Transverse approximation order for i^{th} displacement component
$\mathbf{u}_{3D}$	Exact (three dimensional) solution to the problem considered
$\mathbf{u}_M$	Exact solution of the model
$\mathbf{u}_h^M$	Finite element solution of the model
$\mathbf{e}_h$	Discretization error
$\mathbf{e}_M$	Modeling error
κ_Ω^M	Global modeling effectivity index
$\|\mathbf{u}_{EQ}\|_{E(\Omega)}$	Energy of the finite element solution for equivalent model
$\|\mathbf{u}_{LM}\|_{E(\Omega)}$	Energy of the finite element solution for layerwise model
$\|\mathbf{e}\|_{E(\Omega)}$	Exact modeling error energy norm
$\|\mathbf{e}_M^*\|_{E(\Omega)}$	Estimated modeling error energy norm
η	Discretization error tolerance achieved
η_{model}	Modeling error tolerance achieved

*Graduate Student and Students Member.

†Corresponding author (shekhar@iitk.ac.in) Associate Professor and Non Member.

I. Introduction

Layered composite structures are commonly used for the fabrication of critical components in automobile, aerospace and other industries. The analysis of these structures requires a study of layered medium. The three dimensional ($3D$) elasticity equation is computationally expensive. Families of dimensionally reduced (equivalent single layer) plate models are proposed in the literature to alleviate this problem (see,[1,2] for example). These models are incapable of accurately predicting transverse stresses in regions where three dimensional effects are localized (see Figure 1). More refined plate models (e.g. layerwise plate models) are also available in the literature (see,[3] for example). Layerwise models employ standard dimensionally reduced plate model in each layer. The inter laminar displacement continuity (and in some cases transverse stresses as well) is imposed as an additional constraint. Thus, these models can lead to continuous through thickness transverse stresses. These models, in general, are found to accurately predict the transverse stresses. Further, the equilibrium based postprocessing approach for obtaining transverse stresses is found to be very effective for both dimensionally reduced and layerwise models (see[3]) in general. A novel region-by-region modeling approach[4] has been proposed by authors, where a dimensionally reduced model and layerwise model can be put in any region of the domain. The region-by-region modeling approach was found to be computationally as economical as equivalent single layer models and as accurate as layerwise model. A detailed comparison of families of plate models on the basis of pointwise displacement components and state of stress can be seen in.[3]

In[4] the models used in region-by-region approach were chosen judiciously. In this paper, an explicit modeling error indicator following Schwab[5] is developed using the interelement jumps (in finite element implementation) as modeling error indicator. This indicator is used to predict the regions of high modeling error. A methodology is discussed to adapt the higher models (layerwise model without and with additional sublayers) in these regions.

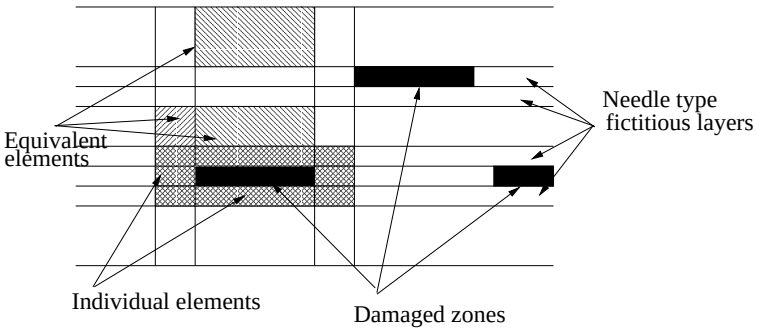

Figure 1. General scenario in laminated composites

II. Plate Models

Analysis of thin laminated structures is based on using predefined director functions in the z-direction, with the displacement field given as a series in terms of products of the director functions and planar functions. Various families of plate models can be defined based on the specific definitions of the director functions. The plate models employed in this study belong to the families of plate models given below.

A. Equivalent Models (EQ)

These are conventionally the most popular plate models, with classical laminate theory and higher order shear deformable models as special cases. The displacement fields corresponding to these models can be defined as:

$$\{u\} = \left\{ \begin{array}{c} u_1(x,y,z) \\ u_2(x,y,z) \\ u_3(x,y,z) \end{array} \right\} = \left\{ \begin{array}{c} \sum_{i=1}^{p_z^1+1} u_{1i}(x,y)\,\phi_i(z) \\ \sum_{i=1}^{p_z^2+1} u_{2i}(x,y)\,\psi_i(z) \\ \sum_{i=1}^{p_z^3+1} u_{3i}(x,y)\,\zeta_i(z) \end{array} \right\} \tag{1}$$

Here, p_z^i, $i = 1, 2, 3$ is the order of the polynomial director functions in the z-direction for u_1, u_2 and u_3, respectively. Generally $p_z^1 = p_z^2$ is chosen. Here, z is the chosen with respect to the middle plane of the plate. Note that for isotropic plates and also for symmetric laminates subjected to transverse loads, $u_1(x,y,z)$ and $u_2(x,y,z)$ are antisymmetric, while $u_3(x,y,z)$ is symmetric with respect to z. Hence, following Schwab,[5] $p_z^1 = p_z^2 = 1$ and $p_z^3 = 0$ is chosen as the first order shear deformable theory. This is represented as the $(1,1,0)$ model. The $HSDT$ model is generally taken as $(3,3,0)$. The director functions are polynomials defined over the full thickness. Following Schwab,[5] a natural hierarchy of such models is given by (1,1,0), (1,1,2), (3,3,2), (3,3,4),$\cdots\cdots$. These models generally correspond to bending effect (i.e. plate under transverse loading). In the current study, the sequence of models due to Schwab[5] are used. Conventionally, the functions $\phi_i(z) = \psi_i(z) = \zeta_i(z)$ are taken as the monomials z^{i-1}. Here we have taken $\phi_i(z) = \psi_i(z) = \zeta_i(z) = M(\hat{z})$, where $M(\hat{z})$ is the Legendre polynomial based hierarchic shape function (see Figure 2) defined in terms of $\hat{z} = \frac{2}{t}z$, where t is the total thickness of the plate. Members of this family of models will be represented by $EQp_{xy}p_z^1p_z^2p_z^3$, where p_{xy} is the in-plane approximation order.

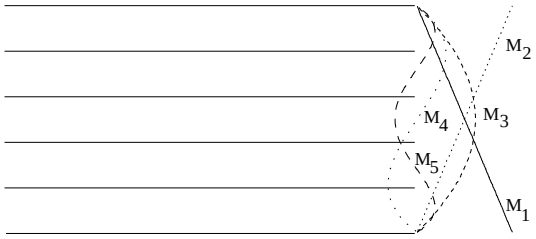

Figure 2. Director approximations over equivalent model

B. Layerwise Models (LM)

This is the most general three-dimensional representation of the displacement field. Each lamina is taken as a separate group and the director functions are defined as the one dimensional basis functions defined over the lamina. From Figure 3, it can be seen that the representation of the displacement field is given by:

$$\{u\} = \left\{ \begin{array}{c} u_1(x,y,z) \\ u_2(x,y,z) \\ u_3(x,y,z) \end{array} \right\} = \left\{ \begin{array}{c} \sum_{i=1}^{n_1} u_{1i}(x,y)\,\bar{M}_i(z) \\ \sum_{i=1}^{n_2} u_{2i}(x,y)\,\bar{M}_i(z) \\ \sum_{i=1}^{n_3} u_{3i}(x,y)\,\bar{M}_i(z) \end{array} \right\} \tag{2}$$

where $n_1 = n_2$ and n_3 depend on the order of approximation $p_z^1 = p_z^2$, p_z^3 and the number of laminae (or layers) nl in the laminate. Hence, here the number of unknowns grows with the number of laminae. Members of this family of models will be represented by $LMp_{xy}p_z^1p_z^2p_z^3$.

The details of equivalent and layerwise model can be seen in.[4,6]

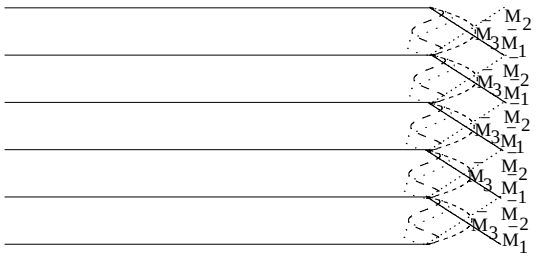

Figure 3. Director approximations over layerwise model

III. Region-by-region Model

In a structural component, the "hot-spots" are generally localized in the vicinity of structural details, boundaries of the domain (faces and edges), re-entrant corners, cut-outs, existing delaminations and ply-failure zones. The solution is unsmooth in the vicinity of these details, while it is very smooth in the remaining part of the domain (see Figures 1 and 4). In order to get an accurate representation of the solution everywhere, it is desirable to use an enriched approximation model (LM or LM with sublaminae if desired) only in the vicinity of the "hot-spot", while in the rest of the domain, a lower order model will suffice. In this study, p_{xy} is uniform over the whole domain, while the approximation enrichment is done by using either a higher value of p_z^i and/or a more refined model, e.g. LM. Thus it is important to build the capability to put any desired model in a specified region, rather than doing an overkill by using a higher model everywhere in the domain (which will be computationally very expensive). This concept has been introduced through the region-by-region modeling approach.

The details of the concept of regions, concept of groups and imposition of constraints and finite element implementation are given in Ref.[4] This concept was a generalization of the planar constrained approximation approach of Demkowicz et al[7] and the $h-d$ approach of Stein et al.[8]

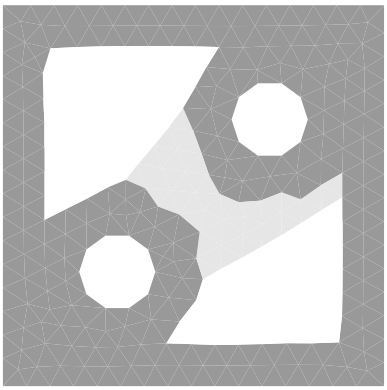

Figure 4. A typical plate domain with cut-outs

IV. Modeling Error Estimation and Control

Let us introduce the terminology for various solutions of the system of laminated plates as:

$\mathbf{u}_{3D}$: the exact (three dimensional) solution to the problem considered

$\mathbf{u}^M$: the exact solution for the model considered

$\mathbf{u}_h^M$: the finite element solution of the model

Then the error in the exact solution and finite element solution ('total error') is given as:

$$\text{total error} = \mathbf{u}_{3D} - \mathbf{u}_h^M = \mathbf{u}_{3D} - \mathbf{u}^M + \mathbf{u}^M - \mathbf{u}_h^M = \left(\mathbf{u}_{3D} - \mathbf{u}^M\right) + \left(\mathbf{u}^M - \mathbf{u}_h^M\right) \tag{3}$$

The first bracketed term on the right hand side denotes the error in the exact solution to the actual problem and exact solution to the model used and second term denotes the error in the exact solution to the model and its finite element approximation. The first term is called as 'modeling error' ($\mathbf{e}_M$) and second term as discretisation error ($\mathbf{e}_h$). Thus,

$$\text{total error} = \mathbf{e}_M + \mathbf{e}_h \tag{4}$$

Thus, equation (4) means that a proper analysis of these structures would require simultaneous control of modeling and discretisation error. In this study, it is assumed that an appropriate initial model is chosen. This plate model is fixed and the discretization error will be measured with respect to the exact solution of the fixed plate model. The models are fixed a-priori in the regions. In this study, an equivalent model in whole domain is used as the starting model. The discretization error is estimated using the patch recovery based a-posteriori error estimator and controlled by using either focussed adaptivity in the quantity of interest or global energy norm as developed by the authors in.[3, 6] Here, it is assumed that the discretization error has been reduced significantly (with respect to modeling error). Then the total error with respect to the fixed model and the new adapted mesh (in some norm) is given by:

$$\|\mathbf{u}_{3D} - \mathbf{u}_h^M\| \approx \|\mathbf{u}_{3D} - \mathbf{u}^M\| \tag{5}$$

Equation (5) assumes that the dominant part of the remaining error is due to the model. The error can be estimated using a residual type error estimator. Since a major goal of this analysis is to develop a quick but sufficiently robust estimator for the modeling error, in the following section an explicit type modeling error indicator is proposed following Schwab.[5] In this study, the modeling error indicator exploits the fact that the equilibrium based postprocessed transverse stresses are generally accurate. Hence, the error estimator is developed using the postprocessed stress state.

Given the model and the approximation for the model, the equilibrium based postprocessed stress state as an indicator of the obtained stress in an element, is employed. The equilibrium equations are given as

$$\begin{aligned} \sigma_{xx,x} + \sigma_{xy,y} + \sigma^*_{xz,z} &= 0 \\ \sigma_{xy,x} + \sigma_{yy,y} + \sigma^*_{yz,z} &= 0 \\ \sigma_{xz,x} + \sigma_{yz,y} + \sigma^*_{zz,z} &= 0 \end{aligned} \tag{6}$$

where σ^*_{xz}, σ^*_{yz} and σ^*_{zz} are obtained from postprocessing (integration with respect to z) of $\sigma_{xx,x}$, $\sigma_{xy,y}$, $\sigma_{xy,x}$ and $\sigma_{yy,y}$.

Given this state of stress in an element τ, the error satisfies:

$$\left(\sigma^{ex}_{xx,x} + \sigma^{ex}_{xy,y} + \sigma^{ex}_{xz,z}\right) - \left(\sigma_{xx,x} + \sigma_{xy,y} + \sigma^*_{xz,z}\right) = \sigma^{er}_{xx,x} + \sigma^{er}_{xy,y} + \sigma^{er}_{xz,z} = 0 \tag{7}$$

where the superscripts ex denotes the exact values and er denotes the error. Similarly, the other two equilibrium equations give

$$\begin{aligned} \sigma^{er}_{xy,x} + \sigma^{er}_{yy,y} + \sigma^{er}_{yz,z} &= 0 \\ \sigma^{er}_{xz,x} + \sigma^{er}_{yz,y} + \sigma^{er}_{zz,z} &= 0 \end{aligned} \tag{8}$$

in the interior of each element, while at the domain boundary, the error satisfies

$$\vec{T} - \vec{T}_{FE} = \bar{T}_{er} \tag{9}$$

where $\vec{T}$ is the actual applied traction and $\vec{T}_{FE}$ is the postprocessed traction computed from finite element solution. In the interior of the domain an element τ has following five interfaces:

1. Top and bottom interface (2 faces) and
2. Lateral interface (3 faces)

At the top and bottom of the element interfaces the transverse stress components are continuous as the state of stress used is computed from equilibrium based postprocessing. Thus, for the transverse components

$$\vec{J}|_{\partial\tau_{transverse}} = \sigma^{\tau}_{i3} n_3 - \sigma^{\tau *}_{i3} n_3 = \mathbf{0} \tag{10}$$

where $\vec{J}|_{\partial\tau_{transverse}}$ denotes the jump on transverse faces. For the lateral faces

$$\vec{J}|_{\partial\tau_{lateral}} = \sigma^{\tau}_{ij} n_j - \sigma^{\tau *}_{ij} n_j \tag{11}$$

where $\vec{J}|_{\partial\tau_{lateral}}$ denotes the jumps in the tractions at the lateral interfaces and τ^* denotes the element sharing the corresponding face of element τ. It is observed that on all lateral faces the jumps are not zero.

It is assumed that the postprocessed stresses leads to $\vec{T} - \vec{T}_{FE} = \mathbf{0}$ in the limit, that is, as the model is refined $\sum_{\partial\tau} |\vec{J}|_{L_2} \to 0$. The modeling error $\mathbf{e}^*_M$ can be obtained by solving

$$\mathcal{B}(\mathbf{e}^*, \mathbf{v}) = \sum_{\tau} \int_{\tau} \sigma^*_{ij}\, \varepsilon_{ij}(\mathbf{v})\, dS = \sum_{\Gamma_i} \int_{\Gamma_i} \vec{J}_{\Gamma_i} \cdot \mathbf{v}\, dA + \sum_{\Gamma^k_{top,\,bottom}} \int_{\Gamma^k} \left(\vec{T} - \vec{T}^*\right) \cdot \mathbf{v}\, dA \tag{12}$$

Note that at the bottom of the domain the known state of transverse stress is used as the boundary condition for the error problem. Hence, in the elements whose bottom face lies on the domain boundary, $\vec{T} - \vec{T}_{FE} = \mathbf{0}$ (as the postprocessed stress uses the known value of traction on this face as the initial values, for integration through the depth). Thus, the error problem uses the mismatch between the specified traction and the postprocessed traction on the top face only.

The Eq. (12) is written as:

$$\mathcal{B}(\mathbf{e}^*_M, \mathbf{v}) = \mathcal{F}(\mathbf{v}) \tag{13}$$

where $\mathbf{e}^*_M$ denotes the estimated modeling error. From Eq. (13),

$$\|\mathbf{e}^*_M\|_{E(\Omega)} = \sup_{\mathbf{v}\in H^1} \frac{|\mathcal{F}(\mathbf{v})|}{\|\mathbf{v}\|_{E(\Omega)}} \leq \sup_{\mathbf{v}\in H^1} \frac{\sum_{\Gamma_i} |\vec{J}_{\Gamma_i}|_{L_2} |\mathbf{v}|_{L2}}{\|\mathbf{v}\|_{E(\Omega)}}$$

$$\leq \sup_{\mathbf{v}\in H^1} \frac{\sqrt{\sum_{\Gamma i} |\mathbf{v}|^2_{L_2}}\, \sqrt{\sum_{\Gamma i} |\vec{J}_{\Gamma i}|^2_{L_2}}}{\|\mathbf{v}\|_{E(\Omega)}}$$

$$\leq \sqrt{\sum_{\Gamma i} |\vec{J}_{\Gamma i}|^2_{L_2}}\ \sup_{\mathbf{v}\in H^1} \frac{\sqrt{\sum_{\Gamma i} |\mathbf{v}|^2_{L_2}}}{\|\mathbf{v}\|_{E(\Omega)}} \leq |\vec{J}|_{L_2}\ \sup_{\mathbf{v}\in H^1} \frac{|\mathbf{v}_{\Gamma i}|_{L_2}}{\|\mathbf{v}\|_{E(\Omega)}} \tag{14}$$

where subscript $\|\|_{E(\Omega)}$ denotes the energy norm in the whole domain and L_2 denotes the L_2 norm.

This global statement can be rewritten in an elementwise form by partitioning the jumps on common faces into two parts. Several partitioning possibilities exist, but the simplest form of equal (i.e. $\alpha = \frac{1}{2}$ or half jump is assigned to each of the neighbouring elements) partitioning is employed here to give

$$\|\mathbf{e}_M^*\|_{E(\Omega)} \leq \sup_{\mathbf{v}\in H^1} \frac{\sum_\tau \left(\sum_{\partial\tau} \alpha\, |\vec{J}_{\partial\tau_i\cap\Gamma_i}|_{L_2} |v_{\partial\tau_i\cap\Gamma_i}|_{L_2}\right)}{\| \mathbf{v} \|_{E(\Omega)}} \tag{15}$$

where Γ_i = collection of all element faces (including those on domain boundaries) and $\partial\tau_i$ = faces of element τ (see figure 5). For brevity $\partial\tau_i \cap \Gamma_i$ is denoted by $\partial\tau$ in the following expressions.

$$\|\mathbf{e}_M^*\|_{E(\Omega)} \leq \frac{\sum_\tau \sum_{\partial\tau} \alpha\, |\vec{J}_{\partial\tau}|_{L_2} |\mathbf{v}_{\partial\tau}|_{L_2}}{\| \mathbf{v} \|_{E(\Omega)}} \leq \frac{\sum_\tau \left(\sum_{\partial\tau} \alpha^2\, |\vec{J}_{\partial\tau}|^2_{L_2}\right)^{\frac{1}{2}} \left(\sum_{\partial\tau} |\mathbf{v}_{\partial\tau}|^2_{L_2}\right)^{\frac{1}{2}}}{\| \mathbf{v} \|_{E(\Omega)}} \tag{16}$$

where $\alpha = \frac{1}{2}$ for interior lateral boundaries, $\alpha = 1$ otherwise. Now

$$\sum_{\partial\tau} |\mathbf{v}_{\partial\tau}|^2_{L_2} \leq C_\tau \|\mathbf{v}\|^2_{E(\tau)} \tag{17}$$

where C_τ is given as

$$C_\tau = \sup_{\mathbf{v}\in H^1(\tau)} \frac{\sum_{\partial\tau} |\mathbf{v}_{\partial\tau}|^2_{L_2}}{\|\mathbf{v}\|^2_{E(\tau)}} \approx \sup_{\mathbf{v}\in H^1(\tau)} \frac{\{v\}^T [A]_{N\times N} \{v\}}{\{v\}^T [K]_{N\times N} \{v\}} \tag{18}$$

Here, $\mathbf{v}$ is chosen from a higher finite dimensional space. Here, in this study the highest layer by layer representation ($LMp_{xy}444$) is used.

The Eq. (18) leads to generalized eigenvalue problem as:

$$[A]\{v\} = \lambda\, [K]\{v\} \tag{19}$$

The generalized eigenvalue problem is solved once. The constant C_τ is found as $C_\tau = \lambda_{max}$.

From Eq. (16)

$$\begin{aligned} \|\mathbf{e}_M^*\|_{E(\Omega)}\, \|\mathbf{v}\|_{E(\Omega)} &\leq \sum_\tau \left(C_\tau \|\mathbf{v}\|^2_{E(\tau)}\right)^{\frac{1}{2}} \left(\sum_{\partial\tau} \alpha^2 |\vec{J}_{\partial\tau}|^2_{L_2}\right)^{\frac{1}{2}} \\ &\leq \sum_\tau \left(\|\mathbf{v}\|^2_{E(\tau)}\right)^{\frac{1}{2}} C_\tau^{\frac{1}{2}} \left(\sum_{\partial\tau} \alpha^2 |\vec{J}_{\partial\tau}|^2_{L_2}\right)^{\frac{1}{2}} \end{aligned} \tag{20}$$

that is

$$\|\mathbf{e}_M^*\|_{E(\Omega)} \leq \sum_\tau \left(C_\tau \sum_{\partial\tau} \alpha^2 |\vec{J}_{\partial\tau}|^2_{L_2}\right)^{\frac{1}{2}} \tag{21}$$

The element indicator is defined as

$$\eta_\tau^M = (C_\tau)^{\frac{1}{2}} \left(\sum_{\partial\tau} \alpha^2 |\vec{J}_{\partial\tau}|^2_{L_2}\right)^{\frac{1}{2}} \tag{22}$$

and global estimated modeling error as

$$\|\mathbf{e}_M^*\|^2_{E(\Omega)} = \sum_\tau \left(\eta_\tau^M\right)^2 \tag{23}$$

The global effectivity index is given as

$$\kappa_{\Omega}^{M} = \frac{\|\mathbf{e}_M^*\|_{E(\Omega)}^2}{\|\mathbf{e}\|_{E(\Omega)}^2} \tag{24}$$

where $\|\mathbf{e}\|_{E(\Omega)}$ is exact error.
The modeling error tolerance achieved is given as

$$\eta_{model} = \frac{\|\mathbf{e}_M^*\|}{\sqrt{2\mathcal{U}(u)}} \tag{25}$$

where $\mathcal{U}(u)$ is strain energy for the given plate model.

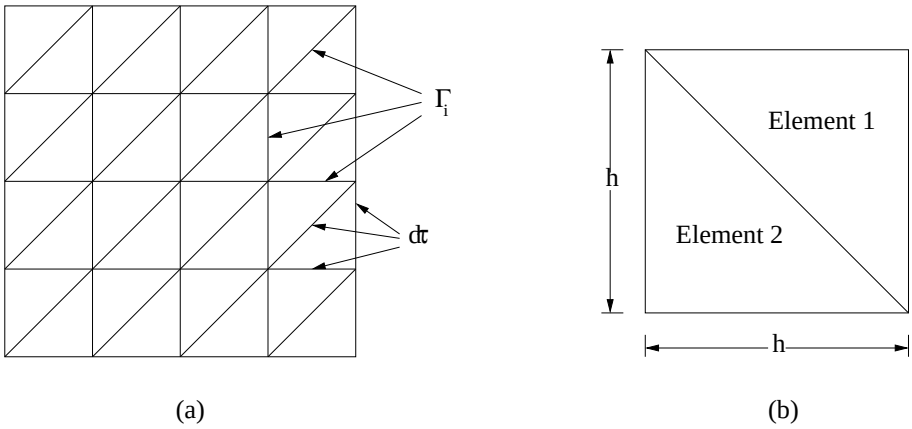

Figure 5. (a) Mesh showing the collection of all element faces (Γ_i) and faces of an element $(\partial\tau_i)$, τ (b) Types of elements used in the meshes for asymptotic behaviour analysis of constant C_τ

V. Numerical Results

In this section, the numerical results are presented to demonstrate the global quality of modeling error estimator proposed. Further, a numerical example is presented to demonstrate the estimation and control of modeling error for a multi-material domain.

A. Global Quality of Error Estimator

The modeling error estimator proposed here has to be tested for reliability. The global quality of the proposed modeling error estimator is tested through effectivity index for two values of length to thickness ratios, S. The effectivity index for $S = 50$, 100 and two boundary conditions (either all edges clamped - CCCC or hard simple supported - HSSSS) are computed for $M55J/M18$ Graphite/Epoxy material (see Table 1). The laminate is subjected to uniform transverse load of intensity $0.025\,N/mm^2$. The mesh used for this study is given in Figure 6. This mesh corresponds to low discretization error ($\eta < 1\%$). The model considered for this study is $EQ3222$. The highest model considered is $LM3444$. For model adaptivity we use $LM3222$ or its variants as the highest possible model.

The global effectivity indices for $[0/90]$ and $[45/-45]$ laminates are given in Tables 2 and 3, respectively. Further, the values of the estimated and (representative) "exact" error, along with the energy of the finite element solution ($\|\mathbf{u}_{EQ}\|_{E(\Omega)}$ and $\|\mathbf{u}_{LM}\|_{E(\Omega)}$) are also reported. From these tables it is seen that:

Table 1. Material properties for $M55J/M18$ and $T300/5208$ Graphite/Epoxy composite

Property	E_{11}	$E_{22} = E_{33}$	$G_{12} = G_{13} = G_{23}$	$\nu_{12} = \nu_{13} = \nu_{23}$	t_i
$M55J/M18$	$280\,GPa$	$6.0\,GPa$	$4.8\,GPa$	0.3	$0.1\,mm$
$T300/5208$	$132.5\,GPa$	$10.8\,GPa$	$5.7\,GPa$	0.24	$0.127\,mm$

1. As the mesh size approaches the thickness of a lamina the quality of effectivity index improves (approaches to value of 1). This can be seen from the values of effectivity index for $S = 50, 100$. For $S = 50$ the mesh size is $h = 0.33\ mm$ and for $S = 100$ the mesh size is $h = 0.66\ mm$.
2. The effectivity index increases for the clamped boundary condition as compared to hard simple supported boundary condition. This can be due to boundary layer effect in the model.
3. The relative modeling error $\left(\sqrt{\frac{\|\mathbf{e}^*_M\|^2}{\|\mathbf{u}_{EQ}\|^2}}\right)$ is small in most cases ($\leq 6\%$) except for $[45/-45]$ laminate with $S = 50$ and all edges hard simple supported (25.5%).
4. The estimator is an upper estimator, i. e. $\kappa_\Omega^M > 1$.

Table 2. Global quality $\left(\kappa_\Omega^M\right)$ of modeling error estimator; $[0/90]$ laminate under uniform transverse load of intensity $0.025\,N/mm^2$ for $M55J/M18$ material

BC	S	$\|\mathbf{e}^*_M\|^2_{E(\Omega)}$	$\|\mathbf{e}\|^2_{E(\Omega)}$	$\|\mathbf{u}_{EQ}\|^2_{E(\Omega)}$	$\|\mathbf{u}_{LM}\|^2_{E(\Omega)}$	$\left(\kappa_\Omega^M\right)$	$\eta\%$
CCCC	50	1.74×10^{-5}	3.83×10^{-6}	5.05×10^{-3}	5.05×10^{-3}	2.13	0.010
	100	6.34×10^{-4}	2.95×10^{-5}	3.13×10^{-1}	3.13×10^{-1}	5.18	0.013
HSSSS	50	3.24×10^{-7}	2.61×10^{-7}	2.92×10^{-2}	2.92×10^{-2}	1.12	8.35×10^{-6}
	100	1.67×10^{-5}	1.59×10^{-5}	1.86	1.86	1.03	2.54×10^{-5}

Table 3. Global quality $\left(\kappa_\Omega^M\right)$ of modeling error estimator; $[45/-45]$ laminate under uniform transverse load of intensity $0.025\,N/mm^2$ for $M55J/M18$ material

BC	S	$\|\mathbf{e}^*_M\|^2_{E(\Omega)}$	$\|\mathbf{e}\|^2_{E(\Omega)}$	$\|\mathbf{u}_{EQ}\|^2_{E(\Omega)}$	$\|\mathbf{u}_{LM}\|^2_{E(\Omega)}$	$\left(\kappa_\Omega^M\right)$	$\eta\%$
CCCC	50	1.68×10^{-5}	2.57×10^{-6}	5.62×10^{-3}	5.62×10^{-3}	2.55	0.013
	100	4.66×10^{-4}	1.84×10^{-5}	3.47×10^{-1}	3.47×10^{-1}	5.03	0.014
HSSSS	50	6.98×10^{-4}	1.30×10^{-5}	1.07×10^{-2}	1.09×10^{-2}	2.32	0.069
	100	1.55×10^{-2}	2.36×10^{-3}	6.75×10^{-1}	6.75×10^{-1}	2.56	0.065

B. Multi-material Domain

Here, [0/90] laminate with all edges clamped and under uniform load of $1\,N/mm^2$ is considered. The plate dimensions are $a = b = 100\,mm$. All the laminae have $T300/5208$ Graphite/Epoxy material everywhere except in 0° layer. In lower right quarter of the 0° lamina the material is replaced by epoxy (see Table 4 for

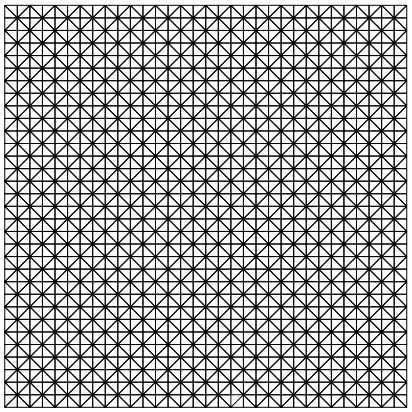

Figure 6. Mesh used for the study of global quality of modeling error estimator

properties). The initial model used is $EQ3333$ in the whole domain. The specified tolerance for discretization and modeling error is 5% each.

Table 4. Material properties for Epoxy

Property	$E_{11} = E_{22} = E_{33}$	$\nu_{12} = \nu_{13} = \nu_{23}$
Value	$6.0\,GPa$	0.36

The initial mesh used is shown in Figure 7(a). The discretization error for this mesh with initial model is 58.2%. The discretization error in the energy is controlled to 0.9%. The corresponding adapted mesh is shown in Figure 7(b). The adapted mesh is fixed.

In the first step of modeling error control procedure, the $LM3333$ model is put in the region shown by dark shading in Figure 7(c). Figure 7(c) and (d) show the normalized modeling error energy density bands in 0° lamina for $EQ3333$ model in whole domain and with adapted model, respectively. The modeling error achieved is 16% and 0.8%, respectively. From this study it can be observed that:

1. The discretization error for $EQ3333$ model with initial mesh is achieved within specified tolerance with discretization error control in energy.

2. The corner formed by epoxy in the 0° lamina acts like a singular edge (in thickness direction) leading to higher modeling error in this region. This is accurately predicted by the proposed modeling error indicator.

VI. Conclusion

The explicit modeling error indicator proposed is implemented successfully. The main features of this study are summarised as follows:

1. The global quality of modeling error indicator is tested. The indicator is found to be robust.

2. The indicator is efficient in predicting the modeling error. The modeling error indicator gives smaller errors as it uses the postprocessed stress for the computation of error.

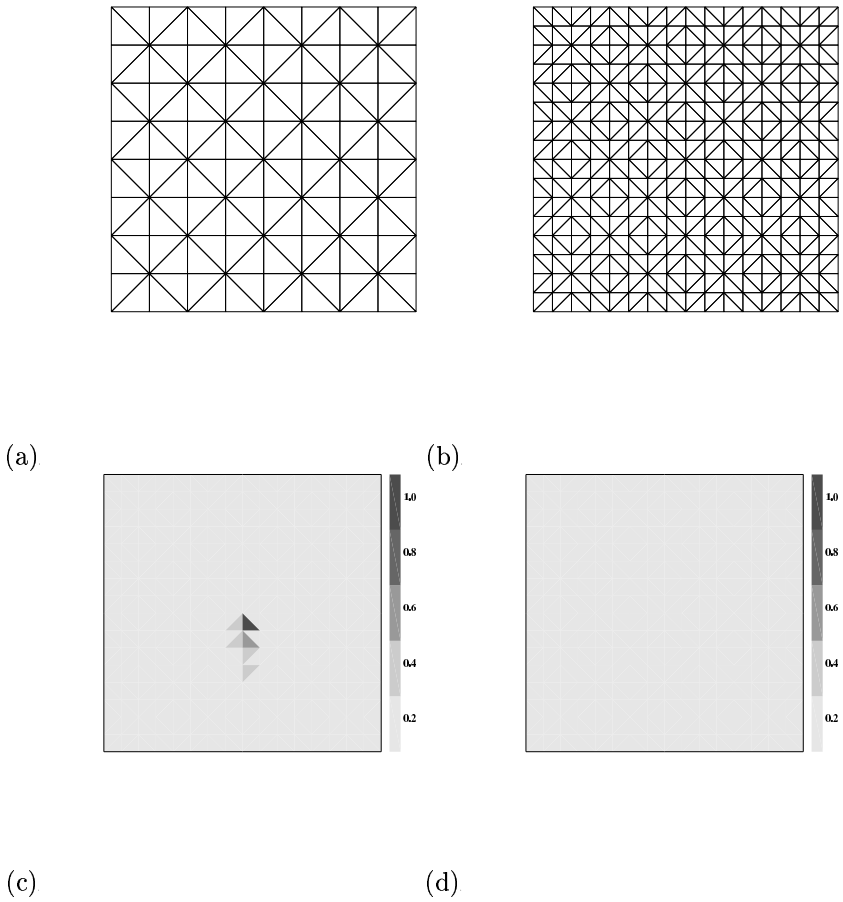

Figure 7. Initial and adapted mesh in (a) and (b); Normalized modeling error density bands in (c) and (d) for [0/90] laminate with all edges clamped; plate dimensions: $a = b = 100\,mm$, $t = 0.254\,mm$; 0° layer with epoxy material in lower right quarter, under uniform load of $1\,N/mm^2$, $T300/5208$ Graphite/Epoxy material

3. The modeling error control methodology is efficient in controlling the modeling error.

References

[1]Reddy. J. N., "A simple higher order theory for laminated composite plates," *Journal of Applied Mechanics, Transactions of ASME*, Vol. 51, 1984, pp. 745, 752.

[2]Babuška. I., Szabó. B. A., and Actis. R. L., "Hierarchic models for laminated composites," *Internatioal Journal for Numerical Methods in Engineering*, Vol. 33, 1992, pp. 503, 535.

[3]Mohite. P. M., and Upadhyay. C. S., "Accurate computation of critical local quantities in composite laminate plates under transverse loading," *Computers and Structures*, Vol. 84, 2006, pp. 657, 675.

[4]Mohite. P. M., and Upadhyay. C. S., "A novel subdomainwise modeling approach for analysis of layered composite structures," 47^{th} AIAA/ASME/ASCE/AHS/ASC *Structures, Structural Dynamics and material Conference*, Newport, Rhode Island 1-4 May, 2006.

[5]Schwab. C., "A-posteriori modeling error estimation for hierarchic plate model," *Numerische Mathematik*, Vol. 74, 1996, pp. 221, 259.

[6]Mohite. P. M., and Upadhyay. C. S., "Reliable computation of local quantities of interest in composite laminated plates," 46^{th} AIAA/ASME/ASCE/AHS/ASC *Structures, Structural Dynamics and material Conference*, Texas, Austin 18-21 April, 2005.

[7]Demkowicz. L., Oden. J. T., Rachowicz. W., and Hardy. O., "Towards a universal $h-p$ adaptive finite element strategy, Part 1. Constrained approximation and data structure," *Computer Methods in Applied Mechanics and Engineering*, Vol. 77, 1989, pp. 79, 112.

[8]Stein. E., Rust. W., and Ohnimus. S., "$h-$ and $d-$ adaptive FE methods for two dimensional structural problems including post-buckling of shells, " *Computer Methods in Applied Mechanics and Engineering*, Vol. 101, 1992, pp. 315, 353.